Dynamic Monolayer Gradients: Active Spatiotemporal Control of Alkanethiol Coatings on Thin Gold Films

Roger H. Terrill,† Karin M. Balss, Yumo Zhang, and Paul W. Bohn*

Department of Chemistry, Beckman Institute and Materials Research Laboratory University of Illinois at Urbana-Champaign 600 South Mathews Avenue, Urbana, Illinois 61801

Received September 23, 1999

The chemical modification of coinage metal surfaces with ω-functionalized alkanethiols has proven to be a popular system for studies of wetting,[1−3] adhesion,[4−7] chemical affinity,[8−12] and electron transfer.[13−15] Varying the composition of binary hydrophilic−hydrophobic self-assembled monolayers (SAMs) can vary the wetting properties of a surface in a continuous manner,[12,16] a fact that has been exploited to distribute surface-active molecules inhomogeneously under mass-transport control.[17,18] One goal of these experiments is to create surfaces which permit supermolecular objects to be manipulated under external control, as recently demonstrated at air−liquid interfaces.[19]

Here we report chemical potential distributions of alkanethiols, which can be manipulated in both space and time under active electrochemical control. In-plane current passed in a thin (5 nm $\leq d \leq$ 80 nm) Au film of resistivity, $\rho(l)$,[20] and cross-section, A, produces an in-plane potential, $V(x)$,

$$V(x) = V_0 + \int_0^x \frac{i\rho(l)}{A}\,dl \qquad (1)$$

whose magnitude and position, relative to a solution reference couple, can be tuned by adjusting the magnitude of the current, i, and the potentiostat voltage offset, V_0, respectively. Electrochemical phenomena typically produce currents 10^3 smaller than the in-plane current required to achieve, say $\Delta V \sim 500$ mV. However, the voltage noise produced by passing the in-plane current is some 10^4 smaller than the in-plane voltage,[21,22] so electrochemical phenomena can be followed and spatial gradients in electrochemical potential transformed into surface chemical potential gradients.

The electrochemical desorption of alkanethiols in methanolic KOH at potentials $V < -0.8$ V vs Ag/AgCl[23−30] was used to establish static gradients in two-dimensional (surface) chemical potential. A 500 Å Au film was contacted by deoxygenated 0.5 M KOH/5 mM octanethiol (OT) in CH_3OH in a flow-cell configuration, and cyclic voltammetry was performed to verify the potential of the cathodic stripping and anodic adsorption waves, cf. Figure 1.[31] OT gradients were formed during 5-min electrolyses performed with a 15 mV mm^{-1} in-plane potential gradient, as implied by the top and bottom axes in Figure 1. The composition gradient was then captured by rapidly (<1 s) removing the substrate and rinsing with pure solvent. The gradient-coated Au films were re-immersed in 5 mM $HS(CH_2)_2CO_2H$ (MPA) in CH_3OH for ca. 2 min to reassemble a hydrophilic SAM in the bare Au areas exposed by reductive desorption of OT. A 2-component linear gradient in composition, i.e., OT/MPA, wetting properties, and surface energy was thereby created. The

* To whom correspondence should be addressed.
† Current address: Department of Chemistry, San Jose State University, One Washington Square, San Jose, CA 95192-0101.

(1) Tao, Y.-T.; Lin, W.-L.; Hietpas, G. D.; Allara, D. L. *J. Phys. Chem. B* **1997**, *101*, 9732−9740.
(2) Laibinis, P.; Whitesides, G.; Allara, D.; Tao, Y. T.; Parikh, A.; Nuzzo, R. *J. Am. Chem. Soc.* **1991**, *113*, 7152−7167.
(3) Laibinis, P. E.; Whitesides, G. M. *J. Am. Chem. Soc.* **1992**, *114*, 1990−1995.
(4) Tidwell, C.; Ertel, S.; Ratner, B.; Tarasevich, B.; Atre, S.; Allara, D. *Langmuir* **1997**, *13*, 3404−3413.
(5) Mrksich, M.; Grunwell, J. R.; Whitesides, G. M. *J. Am. Chem. Soc.* **1995**, *117*, 12009−12010.
(6) Prime, K. L.; Whitesides, G. M. *J. Am. Chem. Soc.* **1993**, *115*, 10714−10721.
(7) Lopez, G. P.; Albers, M. W.; Schreiber, S. L.; Carroll, R.; Peralta, E.; Whitesides, G. M. *J. Am. Chem. Soc.* **1993**, *115*, 5877−5878.
(8) Arduengo, A.; Moran, J.; Rodriguez-Parada, J.; Ward, M. *J. Am. Chem. Soc.* **1990**, *112*, 6153−6154.
(9) Sayre, C.; Collard, D. *Langmuir* **1995**, *11*, 302−306.
(10) Evans, S.; Ulman, A.; Goppert-Berarducci, K.; Gerenser, L. *J. Am. Chem. Soc.* **1991**, *113*, 5867−5868.
(11) Chailapakul, O.; Crooks, R. *Langmuir* **1995**, *11*, 1329−1340.
(12) Chaudhury, M.; Whitesides, G. *Science* **1992**, *255*, 1230−1232.
(13) Chidsey, C.; Bertozzi, C.; Putvinski, T.; Mujsce, A. *J. Am. Chem. Soc.* **1990**, *112*, 4301−4306.
(14) Finklea, H.; Snider, D.; Fedyk, J.; Sabatani, E.; Gafni, Y.; Rubinstein, I. *Langmuir* **1993**, *9*, 3660−3667.
(15) Sun, L.; Crooks, R. *Langmuir* **1993**, *9*, 1951−1954.
(16) Liedberg, B.; Tengvall, P. *Langmuir* **1995**, *11*, 3821−3827.
(17) Thome, J.; Himmelhaus, M.; Zharnikov, M.; Grunze, M. *Langmuir* **1998**, *14*, 7435.
(18) Chaudhury, M.; Whitesides, G. *Science* **1992**, *256*, 1539−1541.
(19) Gallardo, B. S.; Gupta, V. K.; Eagerton, F. D.; Jong, L. I.; Craig, V. S.; Shah, R. R.; Abbott, N. L. *Science* **1999**, *283*, 57−60.
(20) The resistivity itself is a function of position[21,22] according to the following, $\rho(x) = \rho_0 + \delta(x) + \kappa\Gamma(x)$, where $\delta(x)$ represents a position-dependent stochastic fluctuation in the local resistivty, $\Gamma(x)$ is the surface number density, and κ is a constant that depends on the chemical identity of the adsorbate. However, the stochastic and adsorption terms comprise typically an effect ≤ 5%, so they are neglected in this treatment.

(21) Zhang, Y.; Terrill, R. H.; Tanzer, T. A.; Bohn, P. W. *J. Am. Chem. Soc.* **1998**, *120*, 9969−9970.
(22) Zhang, Y.; Terrill, R. H.; Bohn, P. W. *Anal. Chem.* **1999**, *71*, 119−125.
(23) Widrig, C. A.; Chung, C.; Porter, M. D. *J. Electroanal. Chem.* **1991**, *310*, 335−359.
(24) Widrig, C.; Alves, C.; Porter, M. *J. Am. Chem. Soc.* **1991**, *113*, 2805.
(25) Walczak, M.; Chung, C.; Stole, S.; Widrig, C.; Porter, M. *J. Am. Chem. Soc.* **1991**, *113*, 2370.
(26) Yang, D.-F.; Al-Maznai, H.; Morin, M. *J. Phys. Chem. B* **1997**, *101*, 1158−1166.
(27) Yang, D.-F.; Wilde, C. P.; Morin, M. *Langmuir* **1996**, *12*, 6570−6577.
(28) Zhong, C.-J.; Porter, M. D. *J. Electroanal. Chem.* **1997**, *425*, 147−153.
(29) Zhong, C.-J.; Zak, J.; Porter, M. D. *J. Electroanal. Chem.* **1997**, *421*, 9.
(30) Stevenson, K. J.; Mitchell, M.; White, H. S. *J. Phys. Chem. B* **1998**, *102*, 1235−1240.
(31) In these experiments, 3 mm × 75 mm Au films were deposited onto glass microscope slides and configured with four contacts sealed under epoxy to facilitate immersion of the narrow Au WE's.
(32) The spread of the surface energy gradient over nearly 400 mV in in-plane potential is most likely due to surface roughness of the Au films on glass, as anticipated by Porter and co-workers in ref 41.
(33) The small volume of the SPR flow-cell required the use of a Ag/AgCl quasi-reference electrode prepared by contacting the working solution to a 0.5 M KOH/MeOH solution containing the Ag/AgCl electrode reference with a Au wire.
(34) Surface plasmon images were acquired in the Kretschmann configuration with an expanded and collimated beam of 750 nm radiation from an Ar^+-pumped Ti−Sapphire laser. Imaging was performed with a 512 × 512 pixel CCD camera.
(35) Rothenhäusler, B.; Knoll, W. *Nature* **1988**, *332*, 615−617.
(36) Schmitt, F.-J.; Knoll, W. *Biophys. J.* **1991**, *60*, 716−720.
(37) Fischer, B.; Heyn, S.; Egger, M.; Gaub, H. *Langmuir* **1993**, *9*, 136−140.
(38) Jordan, C. E.; Corn, R. M. *Anal. Chem.* **1997**, *69*, 1449−1456.
(39) The series of images in Figure 2 are numerically subtracted from an original exposure of the biased Au film to cancel a small (relative to the SAM) electroreflectance contribution. The reflection angle was set such that dark regions correspond to OT-covered Au and light regions to bare Au.
(40) The difference in half-widths of the desorption waves in Figures 1 and 2 can be attributed to differences in surface preparation. Figure 2 data were obtained on a carefully annealed evaporated Au film, producing Nernstian width waves with minimal separation. Figure 1 data were acquired on unannealed Au, because the magnitude of the gradient, i.e., $\Delta \cos\theta$, is larger on unannealed Au than on annealed Au.
(41) Weisshaar, D. E.; Lamp, B. D.; Porter, M. D. *J. Am. Chem. Soc.* **1992**, *114*, 5860−5862.
(42) The maximum in-plane field is limited by Joule heating to ca. 10^2 V cm^{-1}. An in-plane potential gradient of this magnitude would necessitate an electrode length of the order of 10's of μm to avoid difficulties with solvent electrolysis and gas evolution.

10.1021/ja993442n CCC: $19.00
Published on Web 01/19/2000

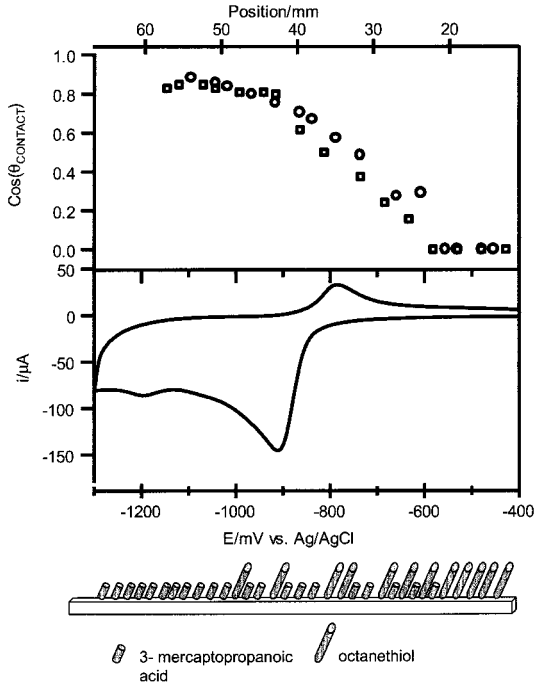

Figure 1. Plot correlating spatial position (top abscissa) and applied potential (bottom abscissa) along a single 60 mm long Au electrode containing a 2-component counterpropagating gradient of OT and MPA. The bottom panel is a plot of the cyclic voltammogram showing how electrochemical phenomena are mapped onto position along the electrode surface. The top panel plots the sessile drop H_2O contact angle vs spatial position (different symbols represent replicate trials). The bottom illustration schematically gives the composition of the 2-component gradient as a function of position, referenced to the distance (top) axis.

transition from the hydrophobic OT to the hydrophilic MPA provided a mechanism for characterizing the SAM gradient. Sessile drop water contact angles were measured as a function of position along the gradient axis, as shown in the top panel of Figure 1. At the spatial extremes of the film contact angles were indistinguishable from those measured on uniform SAMs of either OT or MPA, and a transition region between one-component OT and MPA layers was observed at spatial locations corresponding to potentials of $-600\ \text{mV} \geq V(x) \geq -1000\ \text{mV}$.[32] Interestingly, the onset of the MPA/OT transition (top panel) appears at a potential nearly 200 mV positive of that observed in the 100 mV/s potentiodynamic scan (bottom panel), implying significant kinetic overpotential in the cathodic stripping reaction for OT from the Au on glass substrates used here.

Aside from the relative ease of forming gradients, what sets this approach apart from other gradient-formation techniques,[12,16−18] is the ability to move the gradients in space and time. An example SAM translation is illustrated in Figure 2. The potentiostat was set to an initial offset relative to a Ag/AgCl quasi-reference electrode[33] and sufficient current passed to produce $\Delta V \sim 350$ mV. Then a brightness contrast image of the OT regions of the Au film was obtained using surface plasmon reflectometry[34] (top panels, Figure 2).[35−38] A time series of images was then collected as the offset potential was set to increasingly cathodic values.[39,40] As the potential at the left side of the Au film approaches the equilibrium desorption potential, a light band, corresponding to the loss of OT in this region, appears at the left side of the image along with a gray scale transition from black to white, corresponding to a millimeter-dimension gradient in monolayer adsorbate coverage. The images were recorded at regular intervals, allowing ca. 2 min following the potential steps for diffusion to remove the alkanethiols from the sampling volume of the SPR measurement. Clearly, removal of SAM progresses from the cathodic side of the working electrode as expected. The transition from bare to coated Au appears as a gradient spanning the surface

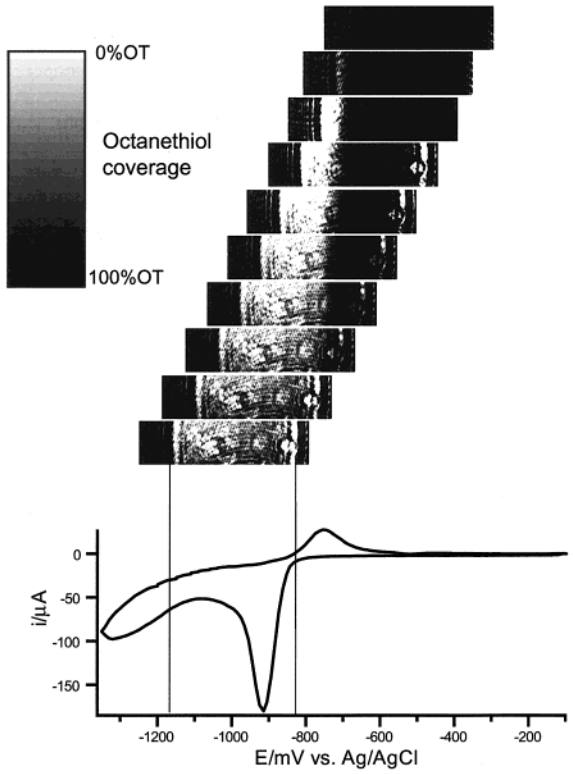

Figure 2. Surface plasma resonance (SPR) images of the same Au electrode in an OT solution with varying potential windows applied. The applied potential for each point along the horizontal axis in each image can be read from the potential directly below it on the *x*-axis of the cyclic voltammogram, as was done explicitly for the right and left ends of the bottom image. SPR images were acquired under conditions in which the resonance (dark areas) corresponds to thiol-covered gold in electrolyte. The physical asperity near the right-hand gasket provides a convenient spatial marker.

region corresponding to ca. $-0.7\ \text{V} \geq V(x) \geq -0.8$ V, potentials intermediate between the oxidative adsorption and reductive desorption potentials in the voltammogram at the bottom.[24,41] The edges of the SAM-covered areas are defined by the gaskets sealing the cell, and a prominent asperity near the right-hand gasket provides a convenient landmark against which the progress of the translating surface gradient can be measured. The ca. 200 mV separation between anodic and cathodic 100 mV/s sweeps reflects both a kinetic and thermodynamic contribution to thiol assembly on these Au films. Correspondingly, the attainable velocity of the advancing front is a function of these kinetics. These data suggest that for thin, annealed Au on glass, surface conditions, and hence boundary advancement, equilibrate with individual potential steps on a subsecond to second time scale and should be even faster for smaller electrode configurations.

For both static and dynamic gradients surface diffusion, not evident at the time and length scales probed in these experiments, will limit the ability to produce surface composition gradients of arbitrary form. Another limit is imposed by the width of the electrochemical waves and the maximum in-plane electrical gradients achievable, estimated to be ca. $10^2\ \text{V cm}^{-1}$.[42] Experiments to exploit these gradients to control the properties, e.g. shape and position of supermolecular objects, are currently underway. Finally we note that although the concept has been demonstrated with electrosorption reactions, the spatial potential gradient scheme can in principle be applied to any electrode reaction, e.g. electrocatalysis, electron-transfer coupled to light absorption/emission, etc.

Acknowledgment. This work was supported by the U.S. Department of Energy through grant No. DE FG02 88ER13949.

JA993442N